GEODYNAMICS & TECTONOPHYSICS
Published by the Institute of the Earth's Crust, Siberian Branch, Russian Academy of Sciences
RECENT GEODYNAMICS

2026 VOLUME 17 ISSUE 4 ARTICLE 0901 ISSN 2078-502X

DOI: 10.5800/GT-2026-17-4-0901

# IDENTIFICATION OF REGIONAL TECTONIC STRUCTURES OF CAMEROON VOLCANIC LINE USING GRAVIMAGNETIC AND 2D LAPLACIAN TERRAIN ANALYSIS TECHNIQUES

**N.E. Ekolle** ✉

Novosibirsk State University, 1 Pirogov St, Novosibirsk 630090, Russia

**ABSTRACT.** Cameroon is made up of an extensive tectonic system that includes a geologically significant structure in Central Africa called the Cameroon Volcanic Line (CVL). In this study, a multi-phase approach was applied to identify new tectonic structures across the CVL using gravity data from the XGM2019e_2159 model, magnetic data from EMAG2, and topographic data from GMRT. First-order and second-order vertical derivatives of both magnetic and gravity data were used to filter geologic structures in the study areas. To understand the trend of the structures based on the potential field, edge enhancement of potential-field data using normalized statistics (standard deviation edge detection) and phase symmetry were applied. Phase symmetry provides phase-based formulation that can detect ridges and valleys corresponding to geological structures regardless of anomaly strength, making it robust to noise and interpolation artifacts. For detailed analysis to delineate new and already existing lineaments, a 2D Laplacian terrain transformation of the topographic data was computed at various heights from 20 to 105 km. The gravitational and magnetic structures discovered were superimposed on the transformed topographic map and drawn out to identify the orientation and direction of the faults. The study further illustrates the occurrence of potential geologic features associated with gravity anomalies, magnetic anomalies, and the new lineaments identified in the area. These results highlight that the lineaments identified are mostly orientated SE-SW and act as evidence of the still continuing process of deformation of the CVL. This finding is essential for advanced regional tectonic modeling across the CVL.

**KEYWORDS:** gravimagnetic anomaly; edge detection; faults; lineaments; 2D Laplacian terrain transformation; CVL

**FUNDING:** Not specified.

EDN: CMGEWK

**RESEARCH ARTICLE**

**Correspondence:** Ndinde Eya Ekolle, ekolleeya@gmail.com

Received: November 23, 2025
Revised: June 22, 2026
Accepted: July 13, 2026

**FOR CITATION:** Ekolle N.E., 2026. Identification of Regional Tectonic Structures of Cameroon Volcanic Line Using Gravimagnetic and 2D Laplacian Terrain Analysis Techniques. Geodynamics & Tectonophysics 17 (4), 0901. doi:10.5800/GT-2026-17-4-0901

# ВЫЯВЛЕНИЕ РЕГИОНАЛЬНЫХ ТЕКТОНИЧЕСКИХ СТРУКТУР КАМЕРУНСКОЙ ЛИНИИ ВУЛКАНОВ С ПОМОЩЬЮ ГРАВИМАГНИТНЫХ НАБЛЮДЕНИЙ И ДВУМЕРНОГО АНАЛИЗА РЕЛЬЕФА ПО ЛАПЛАСИАНУ

**Н.А. Эколл**

Новосибирский государственный университет, 630090, Новосибирск, ул. Пирогова, 1, Россия

**АННОТАЦИЯ.** Камерун представляет собой протяженную тектоническую систему, включающую в себя геологически значимую структуру Центральной Африки – так называемую Камерунскую линию вулканов. Для выявления новых тектонических структур вкрест Камерунской линии вулканов в данном исследовании был применен многостадийный подход с использованием данных модели гравитационного поля Земли XGM2019e_2159, данных модели EMAG2, а также данных цифровой модели рельефа GMRT. Вертикальные производные первого и второго порядка как магнитного, так и гравитационного поля были использованы для выделения геологических структур на изучаемых территориях. Для выделения характерного для структур тренда из данных потенциального поля был применен метод улучшения границ гравимагнитных данных с использованием нормированной статистики (выделение границ стандартного отклонения) и фазового симметрирования. Фазовое симметрирование сделало возможным поэтапное выделение хребтов и долин, соответствующих геологическим структурам независимо от силы аномалий, обеспечивая устойчивость к шуму и артефактам интерполяции. Для детального анализа с целью выделения новых и уже существующих линеаментов было проведено вычисление двумерного преобразования рельефа по лапласиану по топографическим данным на высотах от 20 до 105 км. Выделенные структуры гравитационного и магнитного поля были наложены на преобразованную топографическую карту и отмечены для определения ориентации и направления разломов. В исследовании проиллюстрировано появление потенциальных геологических особенностей, связанных с гравитационными аномалиями, магнитными аномалиями, а также с новыми линеаментами, выделенными на данной территории. Полученные результаты указывают на то, что выделенные линеаменты в основном ориентированы в направлении ЮВ-ЮЗ и свидетельствуют о до сих пор продолжающейся деформации Камерунской линии вулканов. Данное открытие является важным для улучшения регионального тектонического моделирования вкрест Камерунской линии вулканов.

**КЛЮЧЕВЫЕ СЛОВА:** гравиметрическая аномалия; выделение границ; разломы; линеаменты; двумерное преобразование рельефа по лапласиану; Камерунская линия вулканов

**ФИНАНСИРОВАНИЕ:** Не указано.

## 1. INTRODUCTION

The African Plate moves at a speed of 3–7 mm per year from northwest to southwest relative to the Eurasian Plate [Serpelloni et al., 2007; Ebinger et al., 2017]. This movement is consistent with evidence found at the present-day Mid-Atlantic Ridge which shows that the two plates are diverging [Serpelloni et al., 2007]. Africa is one of the highest elevated continent on Earth, largely due to plate tectonics, mantle plumes, and volcanism within the large igneous provinces such as Cameroon Volcanic Line (CVL), East Africa rift valley, Hoggar, Tibesti, and numerous volcanic uplifts [Ebinger et al., 2017]. Previously, geologic studies of Cameroon had tended to use various geological and geophysical methods for identification of new structures, lineaments, rift systems and volcanic activities, as well as for mineral exploration. The Cameroon region is part of a complex that encompasses various tectonic formations, the Congo craton and a major geologic feature in Central Africa known as the CVL [Dumont, 1986; Toteu et al., 2004; Noel et al., 2014]. Many authors studied the systems of tectonic fault zones and the densities of both continental and coastal crustal rocks all over the country using gravity [Koumetio et al., 2014; Nguiya et al., 2018; Ndikum, Tabot, 2023; Ekolle et al., 2025], seismic [Tokam et al., 2010; Goussi Ngalamo et al., 2018], and magnetic [Ndougsa-Mbarga et al., 2014; Cheunteu Fantah et al., 2022] data. However, the tectonic features and lineaments, particularly across the CVL, have been partially identified [Cheunteu Fantah et al., 2022]. The research therein was mostly based on the application of Earth gravitational model EGM 2008, which is somewhat outdated compared to the current XGM2019e_2159. The more accurate XGM2019e_2159 model concerning the global gravitational potential [Zingerle et al., 2020] can therefore increase the reliability in detection of gravity anomaly for the CVL to better delineate and reveal new tectonic structures. Researchers attempted to determine tectonic features of the CVL by combined gravity-magnetic field modeling [Cheunteu Fantah et al., 2022], as well as combined gravimetry-seismic model [Goussi Ngalamo et al., 2018; Kemgang Ghomsi et al., 2021], however, there is a lack of integrated gravity, magnetic and high-resolution topographic data for delineation of structural features associated with the deformation of the CVL.

This study aims to investigate the crustal structure of the CVL by identifying new lineaments (faults) using gravity data (XGM2019e_2159), magnetic data (EMAG2), and topographic data (GMRT). This will provide more details of the structural and geological complex of the CVL.

## 2. TECTONICS AND REGIONAL GEOLOGY

The CVL is defined by a line trending NE-SW through a series of volcanic centers including Mt. Cameroon, volcanic islands of the ocean including Bioko, Principe, São Tome, Annabon, and numerous volcanic seamounts exhibiting seismic activity. These are made up of oceanic island basalts that date back to the end of the Cretaceous period (Late Oligocene / Early Miocene). Volcanic activity along the CVL lacks a clear age progression, with onset ages ranging from ~42 Ma onshore to ~30 Ma offshore, and shows no systematic migration along the line [Meyers et al., 1998; Marzoli et al., 2000; Adams, 2022]. While [Marzoli et al., 2000] observed a NE-SW rejuvenation of peak magmatism within the Western Highlands, Ngaoundere Plateau volcanism does not follow this trend. In [Burke, 2001] interpreted the CVL as related to a mantle plume, but in [Meyers et al., 1998] and most of the subsequent geophysical studies favor an alternative "hotline" model of edge-driven convection without age progression.

The geological basement of Cameroon is shaped by three significant geodynamic events: the Archean orogeny (3.0–2.5 Ga), Eburnean orogeny (2.2–1.8 Ga), and Pan-African orogeny (600–500 Ma). These events led to the splitting of the Precambrian basement rocks into two groups forming the Paleo-, Meso- and Neoproterozoic groups related to the Central African orogenic belt and the Archean Ntem complex associated with the Congo craton [Noel et al., 2014; Mbossi et al., 2026]. The breakup of the continental plates can be interpreted in terms of an anticlockwise movement of the West Africa Plate relative to the South America Plate. Each part of the plate boundary can be said to have a regional breakup stress regime based on its orthogonal and oblique aspects [Lawrence et al., 2002]. This new development in Cameroon has created rocks, grabens, and other tectonic lines that are connected to older ones. Depending on the direction of the lineaments, the fault structures can be divided into three main categories: ESE-WNW, ENE-WSW, and ESE-SSW [Noel et al., 2014].

The CVL lies between the southern craton of the Congo and the northern craton of the Oubanguides, which was formed by the tectonic collision of four different cratons including Congo, West Africa, São Francisco, and a mobile domain in the formation of Gondwana [Castaing et al., 1994; Toteu et al., 2004; Begg et al., 2009; Tokam et al., 2010; Elsheikh et al., 2014]. In our study area, the known fault zones include the Central Africa Shear Zone (CASZ), Central Cameroon Shear Zone (CCSZ), Foumban Shear Zone (FSZ), Sanaga Shear Zone (SSZ), and Pan-African fold belt. This data was obtained from the OneGeology platform (https://onegeology.org/).

The CCSZ – a fault zone located in Cameroon – is an extension of the CASZ. It stretches from Brazil to Sudan. It has been rejuvenated a few times during the Cretaceous dextral movement, before and after the opening of the South Atlantic Ocean [Dorbath et al., 1986]. The CCSZ supports the CVL – a distinctive chain of extinct and active volcanoes: the latter include Mt. Cameroon, Manoun crater lakes, and Nyos [Noel et al., 2014].

The SSZ is part of the CASZ and was previously characterized by dextral motion (probably at the end of the Pan-African orogeny) and a subsequent N-S truncation. It is assumed to be involved in the dextral movement on the northern, mobile part of the zone [Noel et al., 2014].

The CASZ is a huge tectonic area that stretches from Sudan across Central Africa to the Adamawa Plateau in Cameroon [Fairhead, Okereke, 1987]. CASZ extends southwest from the Adamawa Plateau, where it is called the Foumban Shear Zone, and terminates under the southwestern part of Cameroon beneath the CVL, which is a Tertiary-to-Recent line of volcanoes [Tokam et al., 2010].

The FSZ is a mylonite fault found in the central region of Cameroon, stretching for approximately 2000 km from the Cameroonian border to the Sudanese border. This zone

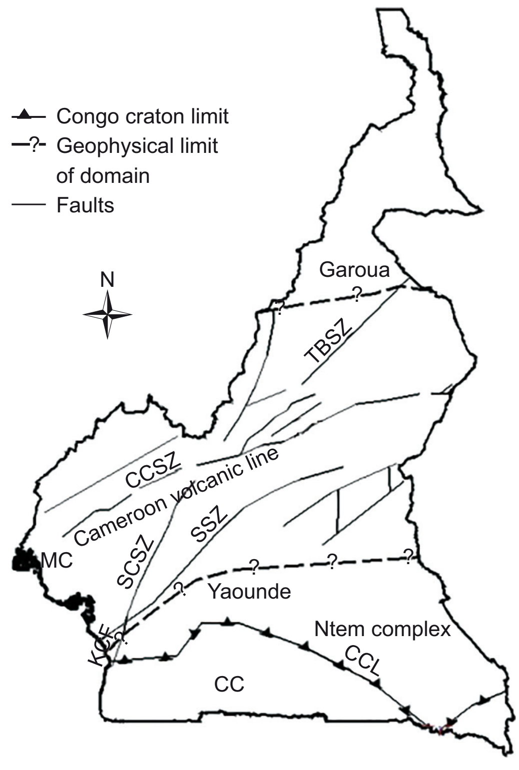


**Fig. 1.** Tectonic framework of Cameroon with major shear zones and fault systems. MC – Mt. Cameroon; SSZ – Sanaga shear zone; KCF – Kribi-Campo fault; SCSZ – South Cameroon shear zone; TBSZ – Tcholliré-Banyo shear zone; CC – Congo craton; CCL – Congo craton limit; CCSZ – Central Cameroon shear zone (after [Noel et al., 2014]).

**Рис. 1.** Тектоническая схема Камеруна, с основными сдвиговыми зонами и системами разломов. MC – влк. Камерун; SSZ – зона сдвига Санага; KCF – разлом Криби-Кампо; SCSZ – зона сдвига Южного Камеруна; TBSZ – зона сдвига Чоллире-Баньо; CC – кратон Конго; CCL – граница кратона Конго; CCSZ – зона сдвига Центрального Камеруна (по [Noel et al., 2014]).

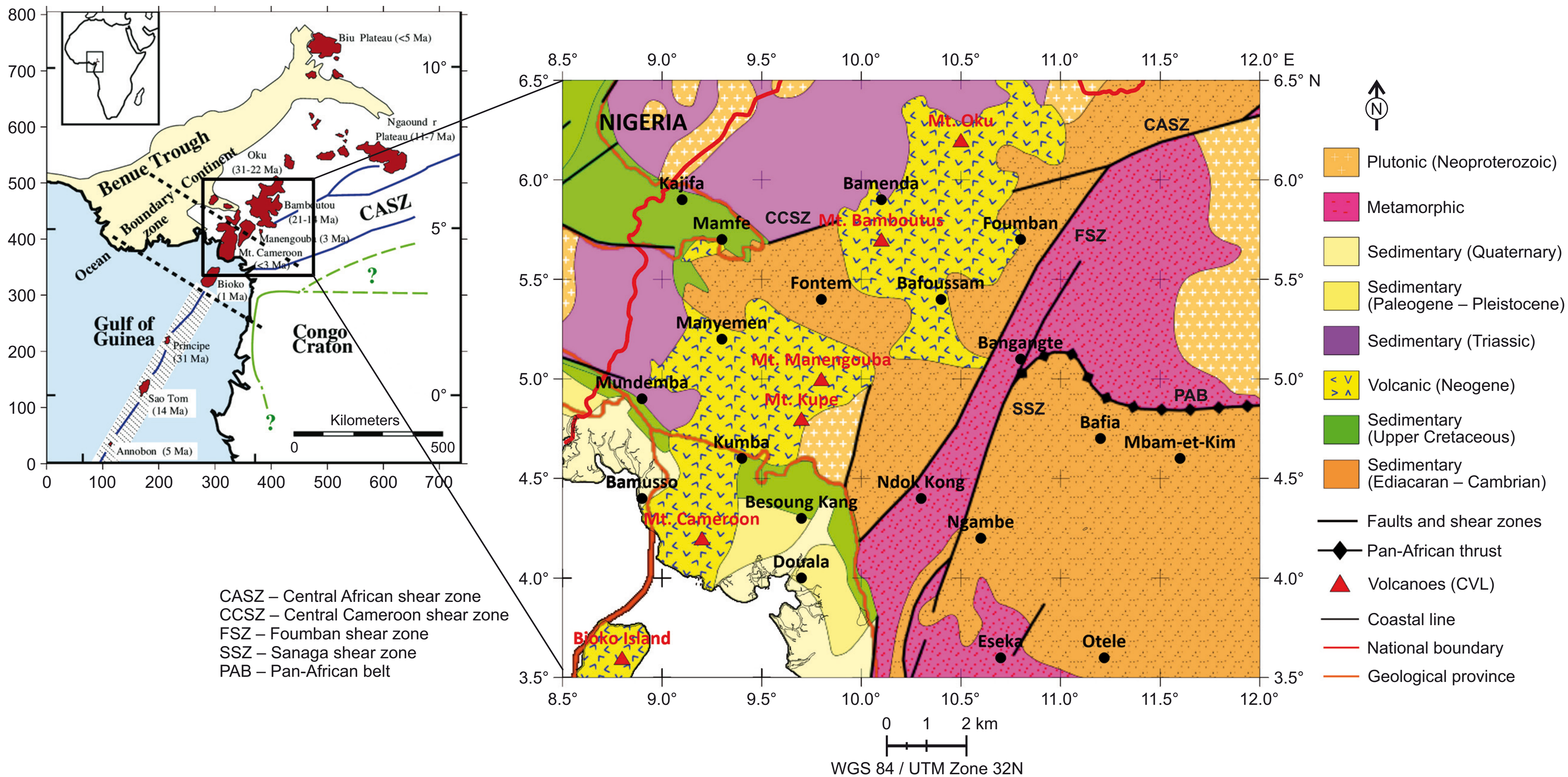


**Fig. 2.** Geological and tectonic map of the CVL [Ekolle et al., 2025].

**Рис. 2.** Геолого-тектоническая карта Камерунской линии вулканов [Ekolle et al., 2025].

makes up part of a large-scale Pan-African fault trending ENE-WSW and is characterized by a dextral displacement of mylonites [Tatchum et al., 2006]. The tectonic map of Cameroon can be seen in Fig. 1.

In the continental part of the CVL, the Pan-African basement rocks are mainly composed of schist and gneiss interrupted by diorite and granite [Fitton, 1987; Déruelle et al., 2007]. As stated by [Tokam et al., 2010], the coastal plain is mainly composed of the Cretaceous sediments (shale, sandstones, and limestone). The volcanic rocks that make up the CVL vary in composition from basalt to trachyte. Some examples include Mt. Etinde (nephelinites), Mt. Oku (rhyolite, quartz, and basalt), Mt. Cameroon (alkaline basalt), Mt. Manengouba (trachyte, rhyolite and basalts), and Mt. Bamboutos (trachyte and alkali basalts).

Mt. Kupe is part of Cameroon's granitic outcrop complexes. It is about 100 km off the coast. There are other volcanic complexes buried beneath huge young basalts of the Mt. Cameroon and Mt. Bioko towards the southwest [Déruelle et al., 1991].

The CVL is mainly found in areas where the fault zones intersect each other [Burke, 2001]. Satellite image-based study, conducted by [Déruelle et al., 1991], discovered a pattern of oblique deformation, which affected the continental crust in the vicinity of the volcanoes on the continental side, and proposed that these volcanoes are within shear zones. This study was conducted across latitudes 3°50' and 6°50' N and longitudes 8°50' and 12°00' E, which is a part of the CVL (Fig. 2).

## 3. DATA AND METHODS

### 3.1. Data

**Topography.** The topography (DEM – Digital Elevation Model) data was downloaded from the Global Multi-Resolution Topography (GMRT; https://www.gmrt.org/GMRT MapTool/) and a topographic map with an elevation of 4000 meters was made (Fig. 3). The coordinate system WGS 84/UTM Zone 32N was used for the map scale.

**Bouguer anomaly.** The Bouguer anomaly maps (Fig. 4) were created using gravity data (XGM2019e_2159) that was downloaded from the ICGEM website (http://icgem.gfz-potsdam.de/home). The grid size (0.02°) was selected prior to using the ICGEM service to do the online Bouguer gravity anomaly data calculations. According to [Marcel et al., 2018; Ekolle et al., 2025], the gridding technique of gravity data yields an interpolated surface that resembles a small, linear elastic layer crossing over every data value with the fewest number of bindings feasible. The final Bouguer anomaly of the study area ranges from –140 to 200 mGal. The regional Bouguer anomaly was subtracted from the final Bouguer anomaly to produce the residual Bouguer anomaly, which ranges from –80 to 180 mGal. By creating the residual anomaly field from the measured gravity field, it is possible to determine the various gravity sources beneath

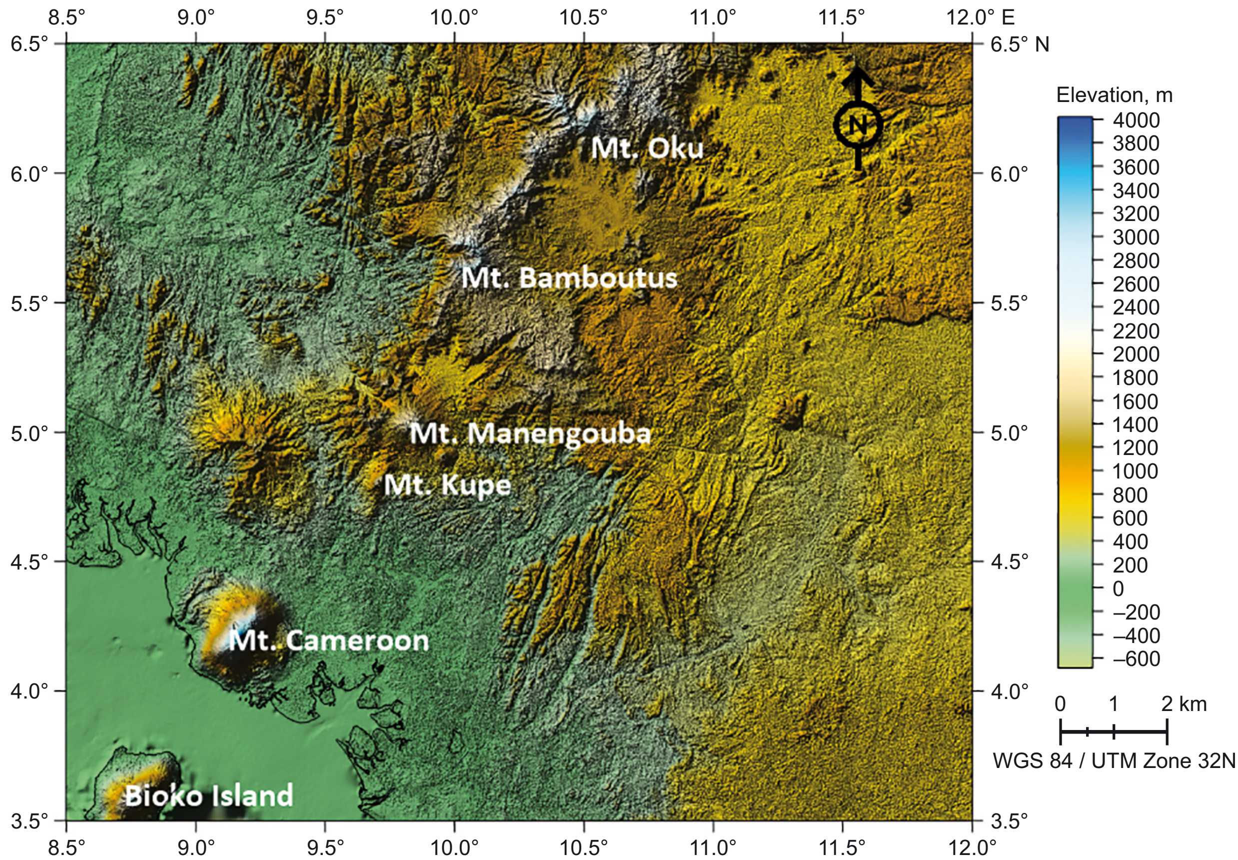


**Fig. 3.** Topographic map of the study area in the CVL.

**Рис. 3.** Топографическая карта изучаемой территории на Камерунской линии вулканов.

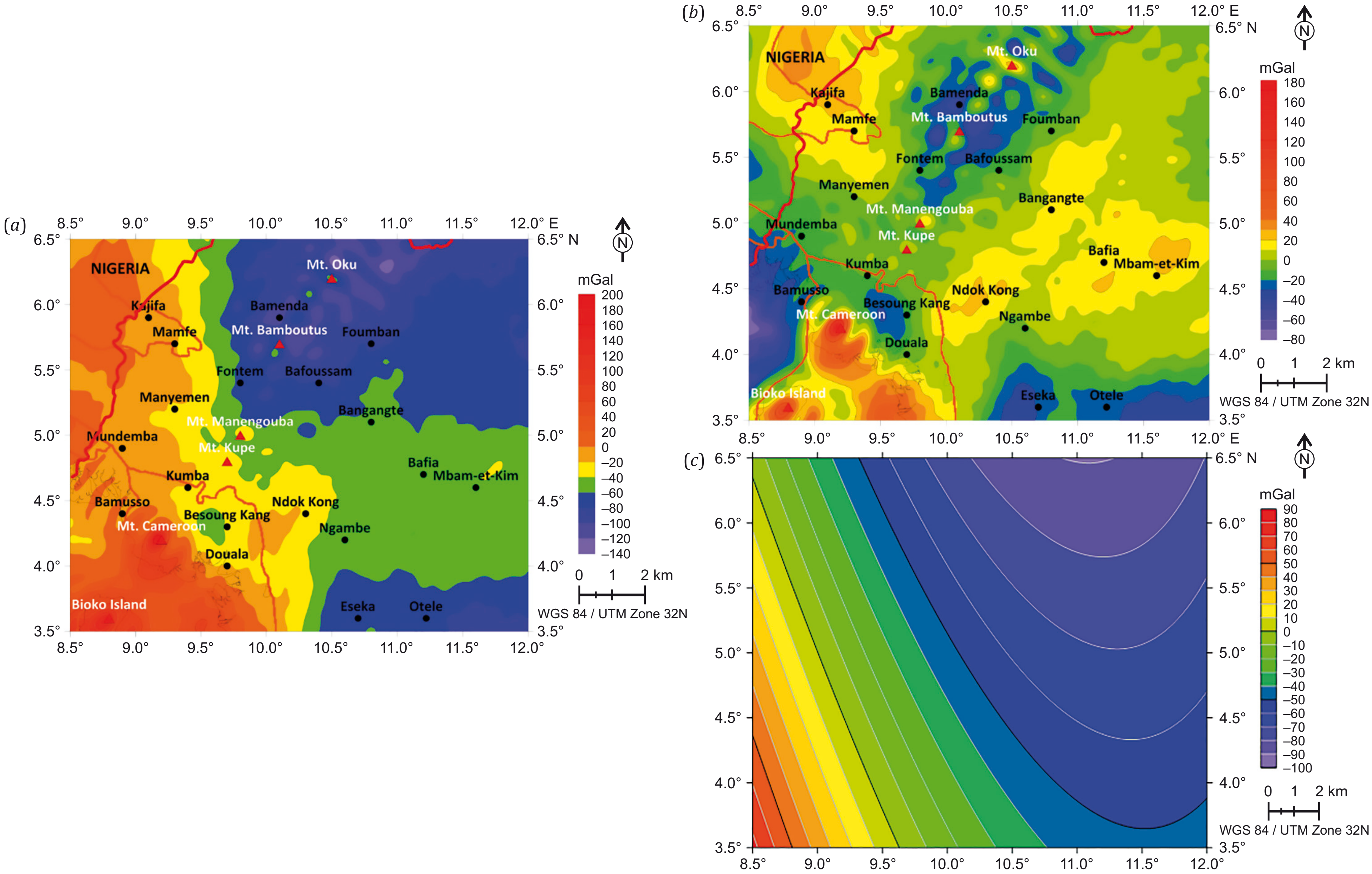


**Fig. 4.** Gravity anomaly maps. (*a*) – Bouguer anomaly; (*b*) – residual Bouguer anomaly; (*c*) – regional Bouguer anomaly.

**Рис. 4.** Карты аномалий силы тяжести. (*a*) – аномалия Буге; (*b*) – остаточная аномалия Буге; (*c*) – региональная аномалия Буге.

the study area that contribute to the characteristics of the Bouguer anomaly map.

**Earth magnetic anomalies grid.** The Earth Magnetic Anomalies Grid (EMAG2) was downloaded from the NOAA website (https://www.ncei.noaa.gov/products/geomagnetic-data). It consists of a 2-arc-min resolution, continued upward at 4 km altitude above sea level. The original data grid consists of airborne, shipborne, and satellite magnetic measurements [Maus et al., 2009]. The total magnetic intensity map (Fig. 5) was created by extracting the grid data for the study area. Some parts located to the northeast of the study area lacked data because no measurements had been recorded. The magnetic intensity ranges from –200 to 65 nT.

Table 1 summarizes the resolution and uncertainty characteristics of the three datasets. The XGM2019e_2159 can resolve crustal-scale faults with offset ~9 km, while EMAG2 is sensitive to shallower, high-contrast magnetic boundaries at similar scales (~8–10 km). The upward continuation of EMAG2 to 4 km altitude [Maus et al., 2009] attenuates signals from sources <2 km depth, limiting resolution of very shallow structures.

### 3.2. Methods

The methodology includes different approaches used for the identification of subsurface lineaments and faults across the CVL. Polynomial regression, kriging, vertical derivatives of the magnetic and gravity fields, edge detector and 2D normalized Laplacian of topographic height were used to reconstruct and reveal ancient tectonic and neotectonic structures through automatic and manual techniques.

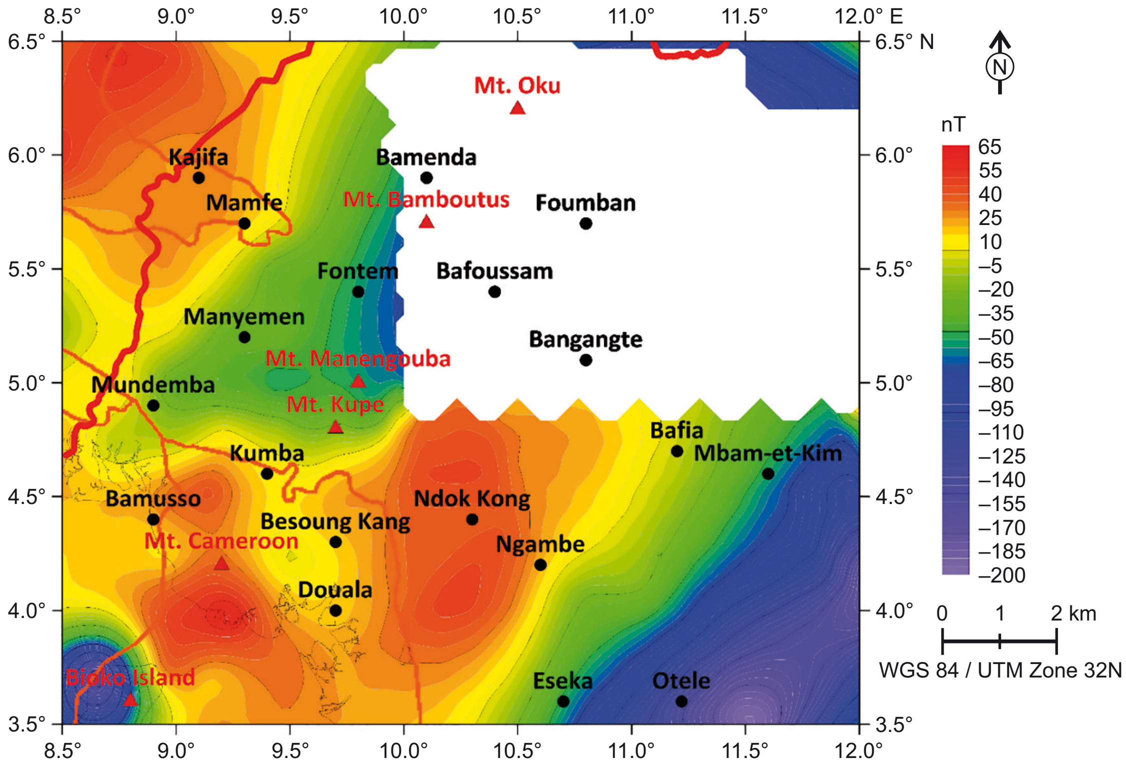


**Fig. 5.** Total magnetic intensity map of the study area.

**Рис. 5.** Карта напряженности магнитного поля изучаемой территории.

**Table 1.** Dataset specifications and uncertainty quantification

**Таблица 1.** Спецификации набора данных и оценка неопределенностей

| Data | Spatial resolution | Vertical accuracy | Horizontal accuracy | Minimum detectable feature | Key limitation |
|---|---|---|---|---|---|
| XGM2019e_2159 | ~9 km (0.08°) | ±2 mGal (global) | ±0.01° | Gravity anomaly with wavelength ≥~9 km | Attenuated short wavelengths over rugged topography |
| EMAG2 | 2-arc-min (~3.7 km) | ±5 nT (oceanic) | ±1 arc-min | Magnetic anomaly with wavelength ≥~8 km | Upward continuation height of 4 km suppresses shallow sources of near-surface volcanoes in CVL |
| GMRT | 15–100 m (variable) | ±10 m (land) | ±15 m | ~50m topographic break | Sparse offshore bathymetric coverage of CVL |

The Bouguer gravity anomaly, total magnetic anomaly, and topography maps were produced using Golden Software Surfer, while the vertical derivative magnetic and gravity anomaly maps were made with Geosoft Oasis Montaj Software. All the maps were created using the same coordinate system-WGS 84/UTM Zone 32N. The gravity data was downloaded in ASCII format (which was the available data format at the time of download, 2023), and then converted into Surfer datafile format before processing the gravity maps. To avoid prediction errors while producing the Bouguer, regional Bouguer and residual Bouguer anomaly maps, kriging interpolation was applied [Kamguia et al., 2008; Gautier et al., 2022; Ekolle et al., 2025]. The second-order polynomial regression was applied on the XGM2019e_2159 data grid to prevent deleting subsurface features within the residual gravity anomalies. This was performed by employing a polynomial regression fitting technique used for gravity data analysis [Kemgang Ghomsi et al., 2021; Ekolle et al. 2025], which allows splitting the Bouguer anomalies between regional and residual anomaly sections. The regional anomalies expand towards the Bouguer anomaly as the degree of the polynomial $n$ increases, revealing additional rock structures in the upper crustal layer.

To help the magnetic fields to extend towards the center of the earth's surface, a Reduction to the Equator (RTE) function was applied. This was accomplished using a similar technique described by [Macleod et al., 1993; Cheunteu Fantah et al., 2022] which has already been shown to be extremely reliable at low latitudes. The RTE has shown effectiveness in correcting the asymmetrical and longitudinal displacement of the recorded overall field strength. The magnetic map was then created using the kriging interpolation approach with RTM data.

**Vertical derivatives.** The first and second vertical derivatives were obtained from the magnetic and gravity grid data, respectively. The derivative filter was used to localize more shallow structures in the study area. Derivatives make the margins of the anomalies more refined, and the shallow structures – more visible or easy to identify [Blakely, Simpson, 1986; Jacobsen 1987; Cheunteu Fantah et al., 2022]. The map of the vertical derivative is much more sensitive to local effects as compared to regional effects. Furthermore, vertical derivative was used to easily detect large-frequency features in the low-frequency or large-amplitude range. When gravity fields from multiple origins are added thereto, it's important to use the derivative filters to separate them and detect their contacts or boundaries [Fedi, Florio, 2001]. The vertical derivative was computed in Fourier domain using the formula:

$$\frac{\partial_g}{\partial_z}(x,y)=F^{-1}\left[|K|\cdot F\left[g(x,y)\right]\right], \quad (1)$$

where $|k|$ – radial wave number, $F$ – Fourier transform, and $F^{-1}$ – inverse Fourier transform.

To reduce noise, the vertical derivative of the potential field at height $h$ was filtered using upward continuation differences given by:

$$VD=\left(\frac{\partial_{\Delta g}}{\partial_z}\right)_{h=0}\approx\frac{\Delta_{g0}-\Delta^{up}_{g\Delta h}}{\Delta h}, \quad (2)$$

where $\Delta g_0$ – original gravity anomaly grid at the measurement level ($h$=0), $\Delta^{up}_{g\Delta h}$ is the field upward continued at the height $\Delta h$, and $\Delta h$ is the difference between the sampling intervals [Fedi, Florio, 2001; Florio et al., 2006].

Magnetic anomaly grid data can be used to create a First Vertical Derivative (FVD) map. This map highlights areas with a quickly changing magnetic anomaly pattern which can show if there are any geological structures like mineralized zones, faults or fractures.

Gravity data was used to delineate faults through anomaly augmentation techniques like Second Vertical Derivative (SVD). The Bouguer gravity anomaly was gridded at approximately 5 km intervals with not more than 20 km circle to generate the initial second vertical derivative gravity map. The Laplace equation was applied to compute the SVD of the vertical component of gravity ($g_z$) in the spatial domain based on horizontal gradients according to [Blakely, 1996; Sumintadireja et al., 2018]:

$$\frac{\partial^2 g_z}{\partial z^2}=-\left(\frac{\partial^2 g_z}{\partial x^2}+\frac{\partial^2 g_z}{\partial y^2}\right). \quad (3)$$

Following potential field theory, equation (3) represents a spatial-domain edge-enhancement operation, not a continuation procedure, and functions as a high-pass filter to delineate the shallow crustal boundaries.

The second horizontal derivative of the gravity field across the x-axis was then used to estimate the second vertical derivative for a larger anomaly across the y-axis with the equation:

$$\frac{\partial^2 g_z}{\partial z^2}\approx-\frac{\partial^2 g_z}{\partial x^2}. \quad (4)$$

Phase symmetry edge-detection filter [Kovesi, 2003; Holden et al., 2016], implemented in Geosoft Oasis Montaj, was applied to automatically identify lineaments based on multi-scale Fourier-phase coherence. This amplitude-invariant method detects ridges and valleys regardless of anomaly strength, making it robust to noise and interpolation artifacts [Holden et al., 2016]. STD filter (Normalized Standard Deviation (NSTD)) was used as a complementary validation filter to confirm edge coherence in high-contrast zones. These techniques provide for more enhancement and detection of edges to delineate the boundaries of subsurface geological structures in the study area [Miller, Singh, 1994; Cooper, Cowan, 2008; Holden et al., 2016]. To minimize the risk of interpolation artifacts being misinterpreted as geological lineaments, only features showing edge-coherence across ≥2 independent processing stages were retained: first and second vertical derivative filtering, NSTD normalization, and phase-symmetry detection. This multi-criteria protocol follows the best approaches for potential-field structural mapping [Cooper, Cowan, 2008; Cheunteu Fantah et al., 2022].

**2D Laplacian topographic height transformation.** This method describes the role of topographic transformation using the Laplacian operator. The Laplacian operator is a fundamental mathematical tool used in many areas of mathematics and science. In the field of image processing, the Laplacian operator is used to detect edges in an image. It can be applied to other measurements, such as topographical elevation, to determine the amount of recharge or discharge in each area. In the field of geoscience, remote sensing, and geomorphology, it can be used to detect ridges, valleys, and tectonic features. It is also used to calculate the curvature of the surface and study the properties of wavelets. It has been widely used in various fields of engineering and science, including geophysics and topography transformation [Glukhmanchuk, Vasilevskiy, 2013; Dobretsov, Vasilevskiy, 2018].

The application of topographic transformation is based on the method of image edge detection [Savant, 2014; Rani, Kumari, 2016]. Laplacian is the measure of the second-order spatial derivative of a 2D-image [Savant, 2014]. Edges characterize object boundaries and are therefore useful for segmentation, marking the boundary between two homogeneous regions [Rani, Kumari, 2016]. For a 2D continuous height $h$ $(x, y)$, the Laplacian function can be given by:

$$\nabla^2 h = \frac{\partial^2 h}{\partial x^2} + \frac{\partial^2 h}{\partial y^2}. \qquad (5)$$

For a DEM raster with 3×3 grid spacing $\Delta x = \Delta y$, finite-difference approximation will be:

$$\nabla^2 h_{i,j} \approx \frac{1}{\Delta^2}\left[h_{i+1,j} + h_{i-1,j} + h_{i,j+1} + h_{i,j-1} - 4h_{i,j}\right], \qquad (6)$$

where $h_{i,j}$ – elevation at grid cell $[i, j]$, $\Delta$ – spatial resolution (equal in $x$ and $y$).

The topography of the study area was transformed using the 2D Laplacian operation function in Golden Software Surfer. This method refined the edges of topographic features and delineated fractured edges present in the study area. This can be seen from different terrain processing methods (see Section 4.3) at different levels of averaging from 20 to 105 km.

## 4. RESULTS AND DISCUSSION

### 4.1. Gravity anomaly

The total Bouguer map (see Fig. 4, a) shows a gravity range of –140 to 190 mGal. The volcanoes towards the north (Mts Oku, Bamboutos, Manenguba, and Kupe) show a relatively negative gravity anomaly ranging from –60 to –10 mGal. The negative value observed can be a result of the regional gravity effect of the less dense rock masses found around the volcanoes and the isostasy effect. Between the Bioko Island and the Mt. Cameroon, including the Atlantic Ocean, lies the biggest positive anomaly of more than 120 mGal was found. This area is made up of basaltic mountains, which is the cause of the positive anomalies therein. The occurrence of igneous rocks on the surface and the thinning of the crust are attributed to the positive Bouguer anomalies found in oceanic regions. In [Poudjom Djomani et al., 1997] indicated that identical mechanisms may have created continental and oceanic crusts in the CVL and that there might be a global uplift due to the buoyant movement of the asthenosphere.

The regional Bouguer anomaly map (Fig. 6) shows the NE-SW trending low to high gravity anomalies, which may indicate that the CVL zone is made up mostly of less dense

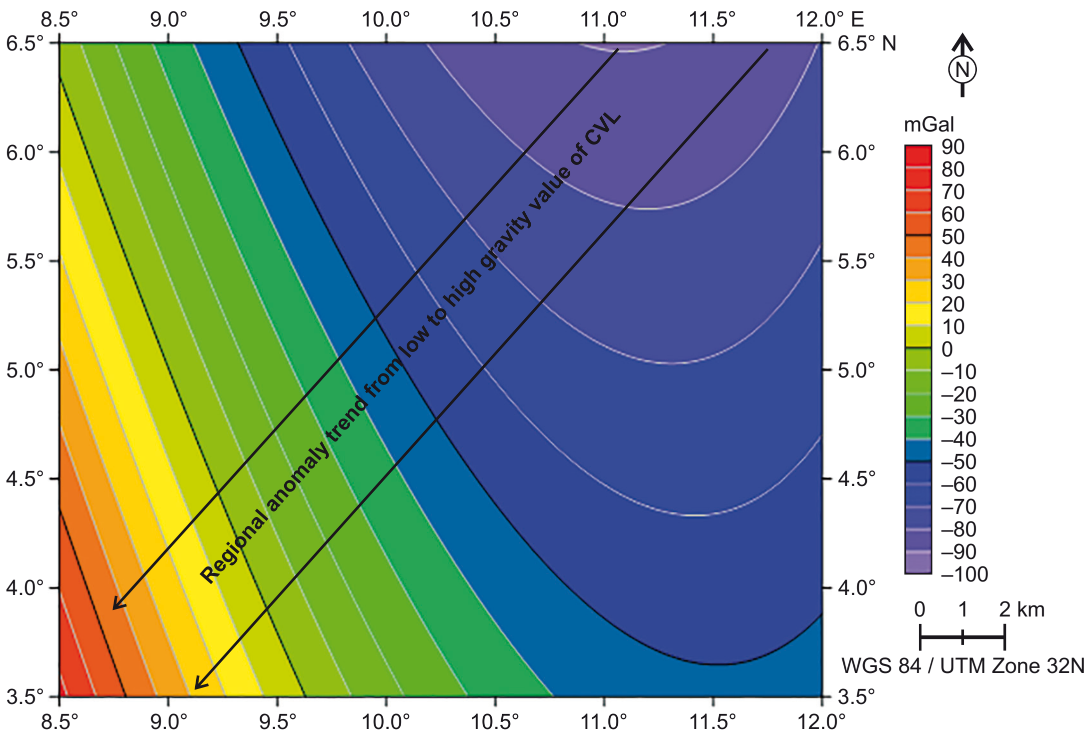


**Fig. 6.** Regional gravity anomaly of the CVL with trend NE-SW.

**Рис. 6.** Региональная гравитационная аномалия Камерунской линии вулканов СВ-ЮЗ направления.

rocks to the north and denser rocks to the south. But the main reason for such behaviour of the regional Bouguer gravity field is isostasy, which leads to the fact that positive Bouguer anomalies are characteristic of all oceanic regions of the Earth, just as negative anomalies are inherent in mountains. The gravity anomaly value ranges from –100 to 90 mGal.

The residual map (see Fig. 4, b) displays clear discontinuities of a high gravity signature of 10 to 40 mGal towards the west around Bafia, Ndok-Kong and Mbam-et-Kim, which were not highlighted before by the total Bouguer anomaly. This is due to the large granitic and gneiss rocks found along the Pan-African thrust [Marcel et al., 2018]. According to [Déruelle et al., 1991, 2007], the Mt. Cameroon does in fact cover dense volcanic formations that date back to between the Cenozoic and the present. At local scales and in the lithosphere's outermost layer, the effect of Bouguer anomalies' refinement is becoming increasingly apparent [Kamto et al., 2020]. The residual anomaly highlighted local features more clearly and revealed the dense rock that forms the volcanoes towards the north, which was not visible on the total Bouguer anomaly map. The volcanoes are represented with a positive anomaly from 0 to 30 mGal. The southern portion of the Benue Trough (Nigeria), which is filled with less dense Cretaceous sedimentary layers, causes the emergence of the NE-SW trending zones associated with significantly negative amplitudes and lies around the Mamfe sedimentary basins of Manyemen and Fontem. Negative zones are usually associated with less dense, intrusive bodies. Zones associated with negative anomalies are found around the Douala basin and Eseka, as well as Otele. These zones emerged due to an early-to-late Cretaceous sediment basin.

The low gravity anomaly values at the Mt. Bamboutos and the Mt. Oku could be a result of deep-seated intrusions that are located at a close distance to the Moho depth, and as such the gravity anomaly is highly influenced by the surrounding less dense sedimentary rock mass cover of Fontem, Bamenda, and Foumban, thereby making the readings lower. Bouguer anomalies over mountainous terrain tend to be negative because they are caused by isostatic equilibrium. The density of rocks beneath mountains is lower than that of adjacent, mantle-derived rocks. The fact that the region has a high negative Bouguer anomaly in the north of the country implies that it is a deep source region [Kenfack et al., 2017].

### 4.2. Magnetic anomaly

The total magnetic intensity map (see Fig. 5) represents areas of high potential for mineral extraction. Three distinct high positive magnetic anomalies can be identified covering different places extending from the Mt. Cameroon and its surroundings to the Atlantic Ocean, the areas of Ndok Kong and Ngambe, and the ground towards the NW boundary between Nigeria and Cameroon. These areas signify a potential of possible mineral deposits. Between latitudes 6.0° and 6.5° N and longitudes 8.5° and 9.0° E, there is a big area of high magnetic anomalies, which range from 40 to 65 nT. These highly positive anomalies are associated with the Benue trough. This reflects similar findings made by [Cheunteu Fantah et al., 2022]. Ndok Kong is in southeastern Cameroon in the same geological belt as Nyong which is close to the Congo craton. This area has large deposits of nickel, cobalt, and manganese, while Ngambe is known for its high potential of iron deposits. The alignment of spots of positive anomalies approximately in the N90°E direction is an indication that the magnetization is influenced potentially by the tectonics. There are similarities between magnetic and gravity anomalies with regard to their direction, concentric shape, and location of their anomaly gradients. Therefore, magnetic approaches can offer extra precision to structural characteristics that are impossible to identify using gravity variations.

### 4.3. Structural results and interpretation

The results presented here include the use of automatic lineament identification for the magnetic intensity map and gravity map. Before the FVD of the magnetic grid data had been applied, the map was reduced to the equator. RTE is the process of increasing the signal of magnetic anomalies detected close to the equator [Cheunteu Fantah et al., 2022]. The magnetic anomaly map was transformed for automatic detection of magnetic lineaments in the study area using Geosoft Oasis Montaj (Fig. 7). This process was more accurately applied to the map of the gravity anomaly for a high-precision observation of lineaments in the study area (Fig. 8). While NSTD can enhance boundary delineation, it is susceptible to directional striping artifacts producing horizontal noise which are due to the filtering effects of weak and strong anomalies at the same intensity [Cooper, Cowan, 2008]. For this reason, Phase symmetry was selected as the primary edge-detection method because its amplitude-invariant and phase-based formulation is robust to interpolation artifacts and grid-aligned noise (see Fig. 7, c; Fig. 8, c). NSTD was retained as a complementary validation filter; lineaments showing coherence across both methods were classified as high confidence in the final interpretation. The mapping and identification of these structures depend on a multi-dimensional assessment of vertical gradient maps of both gravity and magnetic anomalies [Blakely, Simpson, 1986]. Furthermore, the SVD demonstrated strong alignment to geological structures, which, in most cases, indicate possible reverse or normal faults [Ming et al., 2021].

The topography of the study area was transformed by calculating the normalized Laplacian. This provides the added advantage of evaluating more crustal fracture zones and revealing the similarity of the trends of lineaments in the study area. To calculate the Laplacian, different averaging window sizes were used: 20–31 km, 20–40 km, 40–71 km, 75–89 km, and 74–105 km (Figs 9, 10).

The gravitational and magnetic structures discovered (see Figs 7, b, c, 8, b, c) were superimposed on the transformed topographic maps and drawn out to identify the orientation and direction of the lineaments exhibiting similar trends. The lineament map (Fig. 11) was plotted by following the spatial behaviour of the superimposed maxima with depth and the trend of subsurface lineament observed in the different maps. The lineament map was integrated with the known geologic and fault maps to identify new regional tectonic structures in the study area (Fig. 12). This process is vital for validation, showing that the lineaments identified represent actual geological boundaries. In the northeastern sector where EMAG2 magnetic data are unavailable, lineaments were identified solely through coherence between gravity (XGM2019e_2159) and topographic (GMRT) edge signals.

The edges of the anomalies were straightened during correlation representing probable fault zones in the area and newly formed faults of the CVL. The lineaments represented by these combined techniques are comprehensive, given that they require detailed observation and time for reconstruction. However, the effectiveness of the topography transformation is limited by the fact that the image contains some round-edged features that can be referred to as artifacts (see Fig. 10). These artifacts can be clearly seen in Fig. 9 at image grids 40–71 km, 75–89 km, and 74–105 km. Upon closer examination, these artifacts

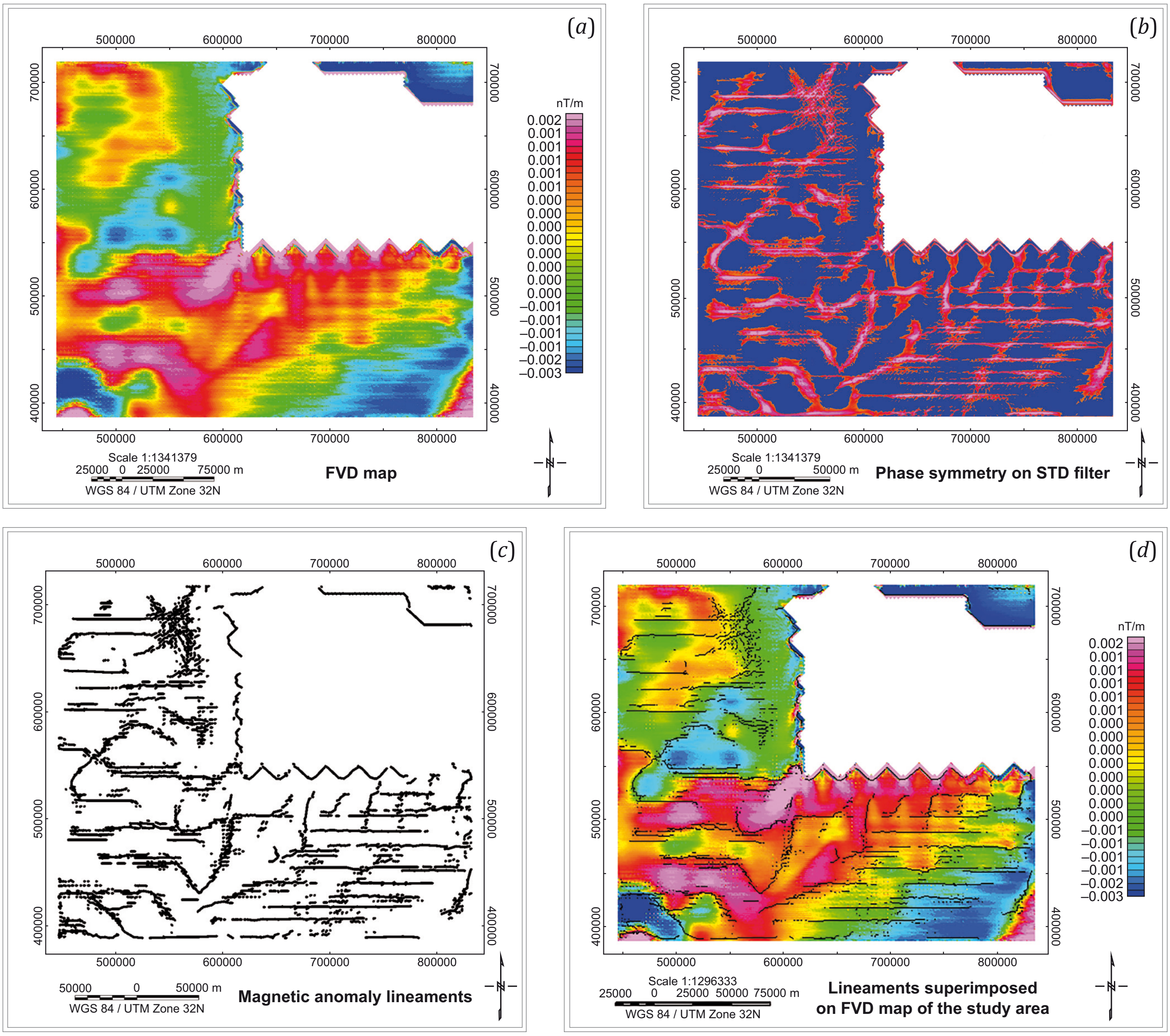


**Fig. 7**. Automatic magnetic lineament identification and the FVD map of the study area.
(*a*) – FVD map; (*b*) – automatic phase symmetry on STD filter; (*c*) – lineament map using phase symmetry edge detection on local spatial frequencies; (*d*) – lineament superimposed on the FVD map.

**Рис. 7.** Автоматическая идентификация магнитных линеаментов и карта первой вертикальной производной (FVD) для изучаемой территории.
(*a*) – карта FVD; (*b*) – автоматическое симметрирование фаз с помощью фильтра на основе стандартного отклонения; (*c*) – карта линеаментов с выделением границ фазового симметрирования на локальных пространственных частотах; (*d*) – линеамент с наложением на карту FVD.

are due to local perturbations of the relief associated with volcanoes.

A total of 52 lineaments were identified (see Fig. 11). Based on statistical analysis (Fig. 13), 15 lineaments (28.8 %) are oriented SE-S and 33 lineaments (63.5 %) are oriented S-SW, which represent the dominant directions. The observed S-SW dominance (63.5 %) aligns with the dextral shear regime of the CCSZ [Dorbath et al., 1986; Noel et al., 2014] and is consistent with asymmetric patterns reported in the previous CVL structural studies [Cheunteu Fantah et al., 2022]. This result indicates that majority of the lineaments in the study area are oriented roughly between southeast and southwest. The observed orientations are controlled by known fault movements and ongoing tectonics of the CVL.

According to a detailed petrological analysis in [Marzoli et al., 2000], the younging trend in the southwest, which extends from the Oligocene volcanism in the northern portion of the Mt. Oku toward the presently active Mt. Cameroon, indicates that the African Plate continues to move over a deep-seated mantle heating anomalous region.

The structural features (see Fig. 11, 12) produced from gravity, magnetics, and topography show a linear fit to the known geological contacts of SSZ and FSZ; other contacts

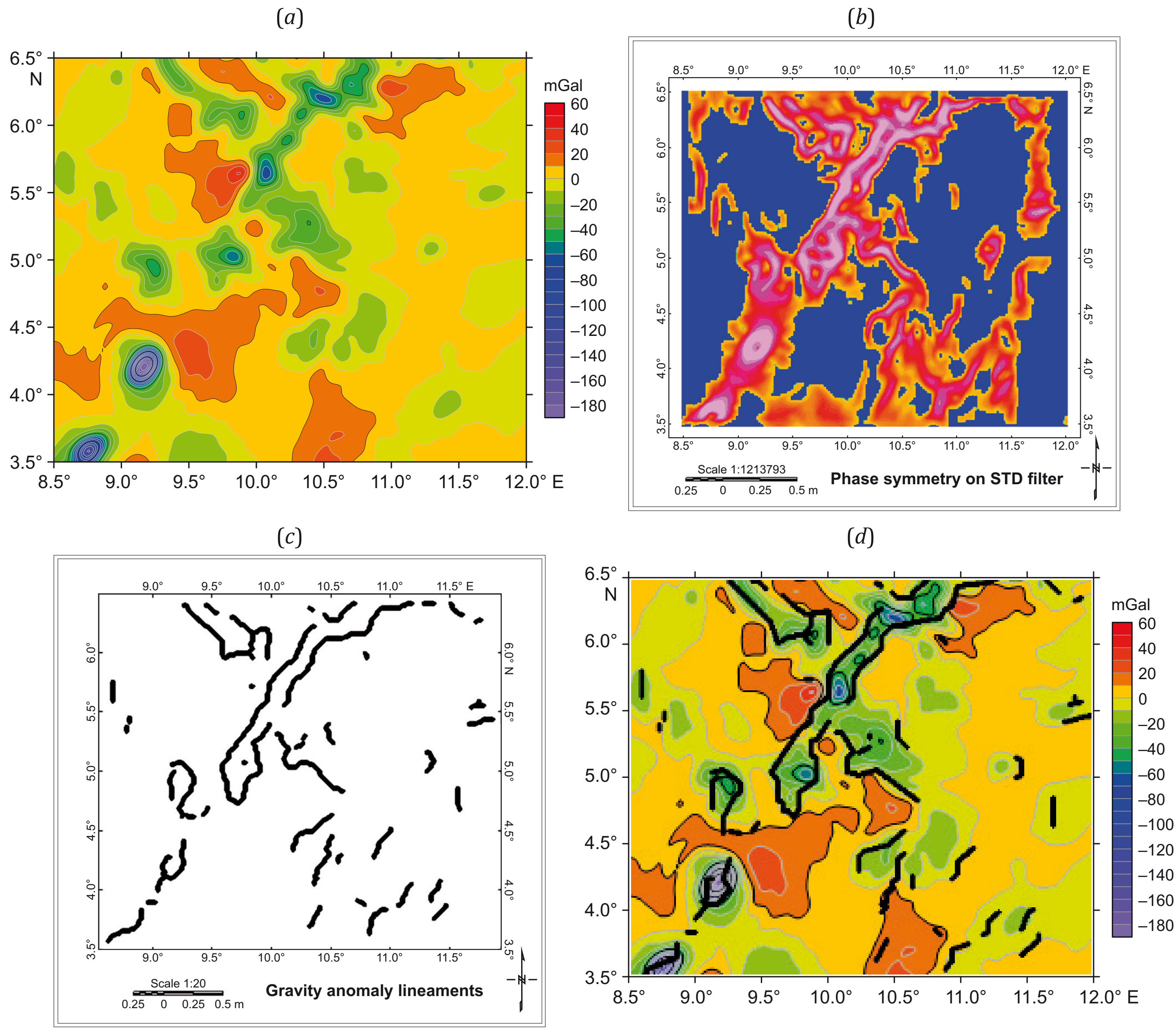


**Fig. 8.** Automatic gravity lineament identification and SVD map.
(*a*) – second vertical derivative gravity map; (*b*) – automatic phase symmetry on STD filter; (*c*) – lineament map using phase symmetry edge detection on local spatial frequencies; (*d*) – lineament superimposed on the second vertical derivative map.

**Рис. 8.** Автоматическая идентификация гравилинеаментов и карта второй вертикальной производной (SVD).
(*a*) – карта второй вертикальной производной; (*b*) – автоматическое симметрирование фаз с помощью фильтра на основе стандартного отклонения; (*c*) – карта линеаментов с выделением границ фазового симметрирования на локальных пространственных частотах; (*d*) – линеамент с наложением на карту SVD.

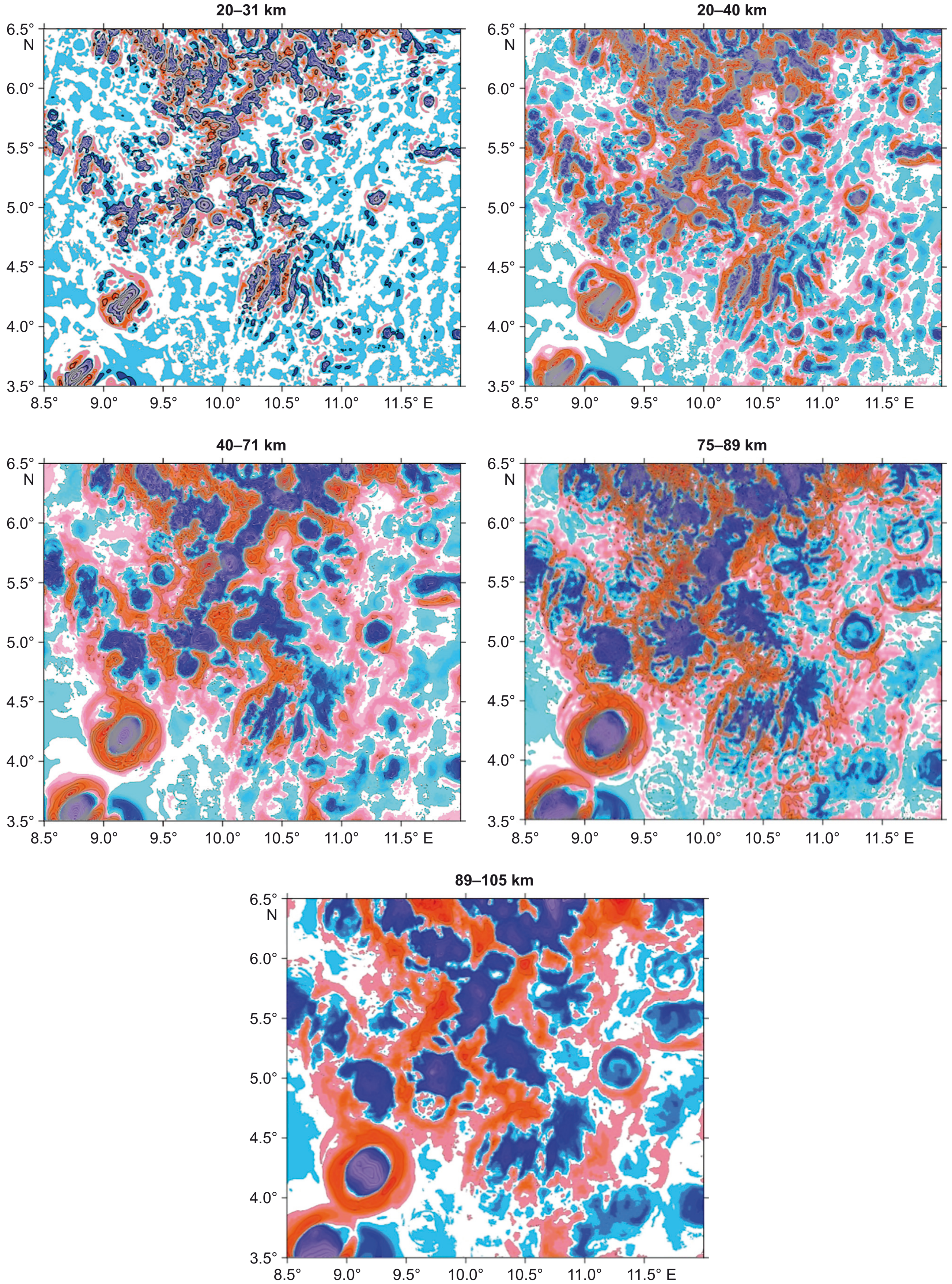


**Fig. 9.** 2D Laplacian topographic transformation of the CVL calculated for different averaging window sizes.

**Рис. 9.** Двумерное преобразование рельефа Камерунской линии вулканов по лапласиану, вычисленное для окон усреднения разных размеров.

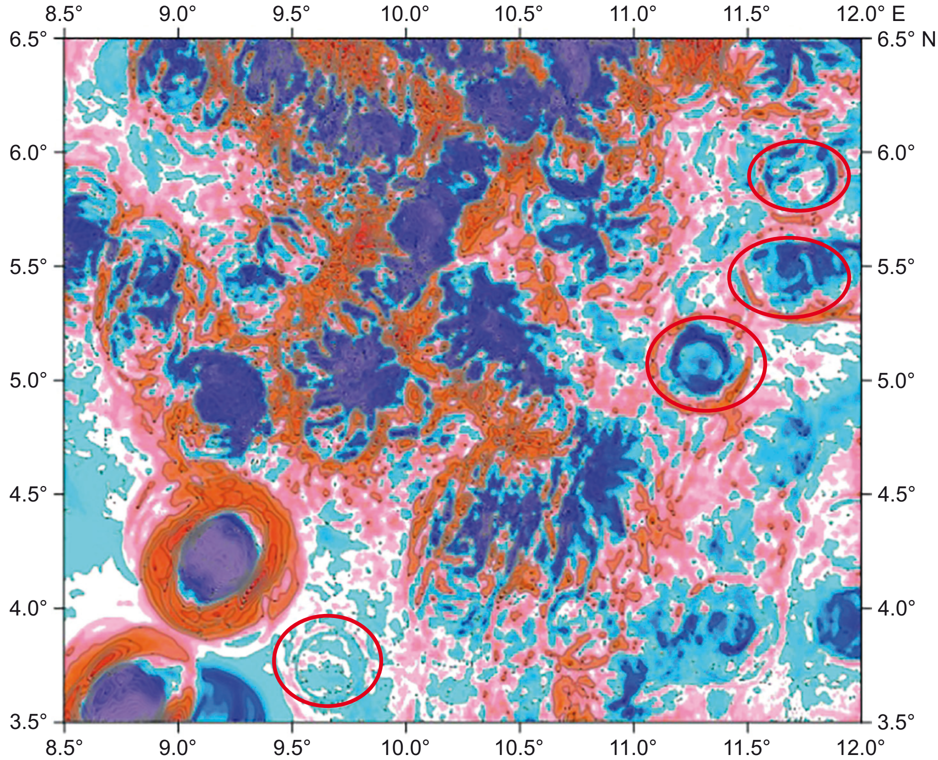


**Fig. 10.** Artifacts present on topographic transformed map.

**Рис. 10.** Артефакты на преобразованной топографической карте.

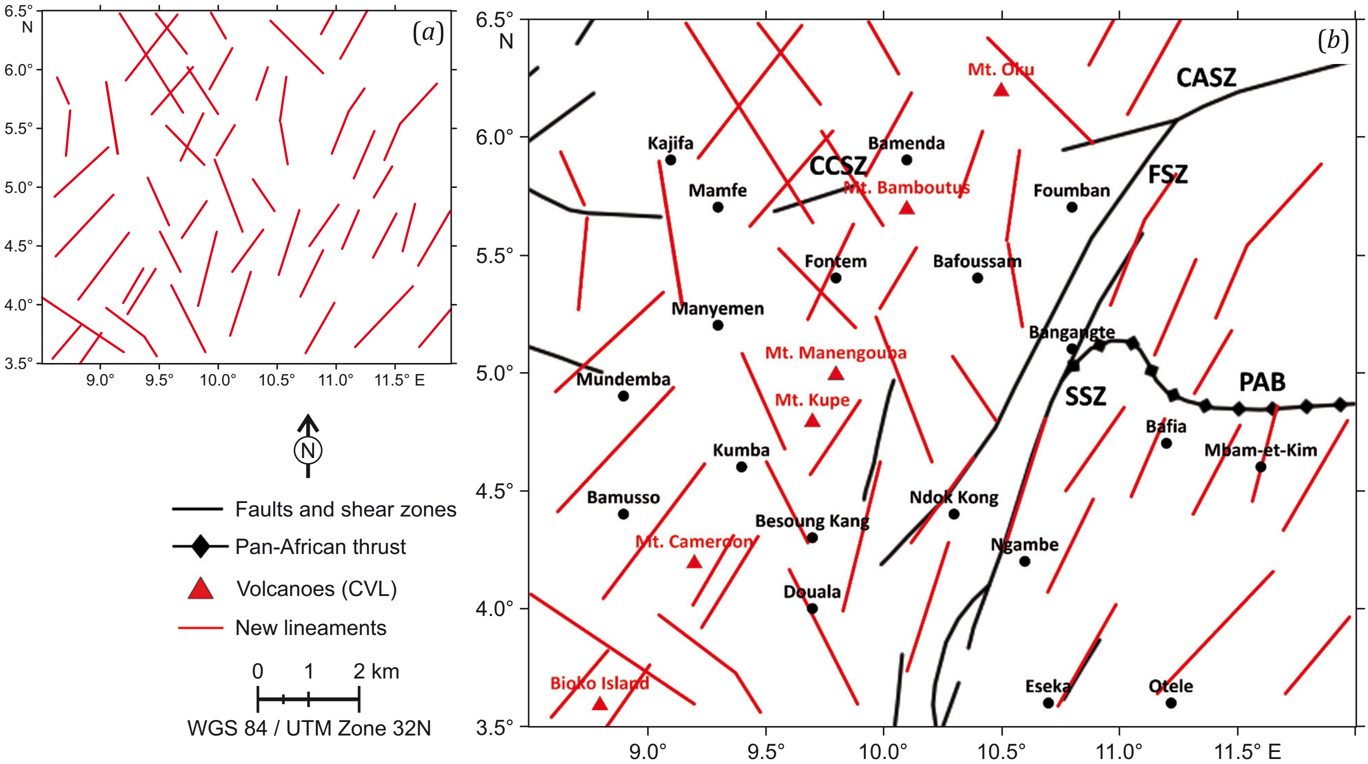


**Fig. 11.** Lineament map of the CVL from magnetic, gravity and transformed topography analysis (*a*), and lineaments with known faults (*b*).

**Рис. 11.** Карта линеаментов Камерунской линии вулканов, составленная на основе магнитного и гравиметрического анализа, а также анализа преобразованного рельефа (*a*), и линеаменты, связанные с известными разломами (*b*).

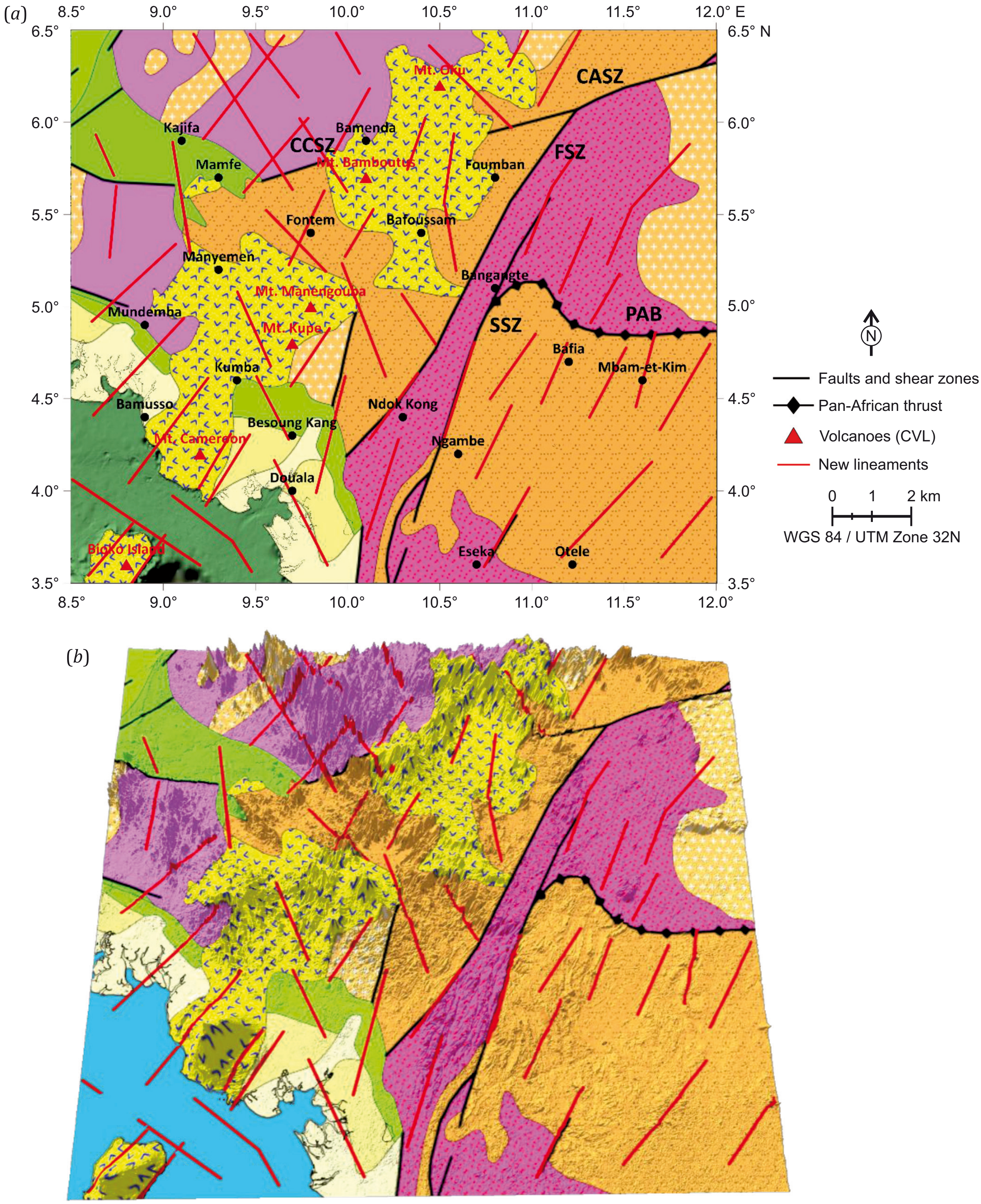


**Fig. 12.** New lineaments, known fault and geology map of the CVL (*a*) and 3D visualization (*b*).

**Рис. 12.** Новые линеаменты, известные разломы и геологическая карта Камерунской линии вулканов (*a*) и 3D-визуализация (*b*).

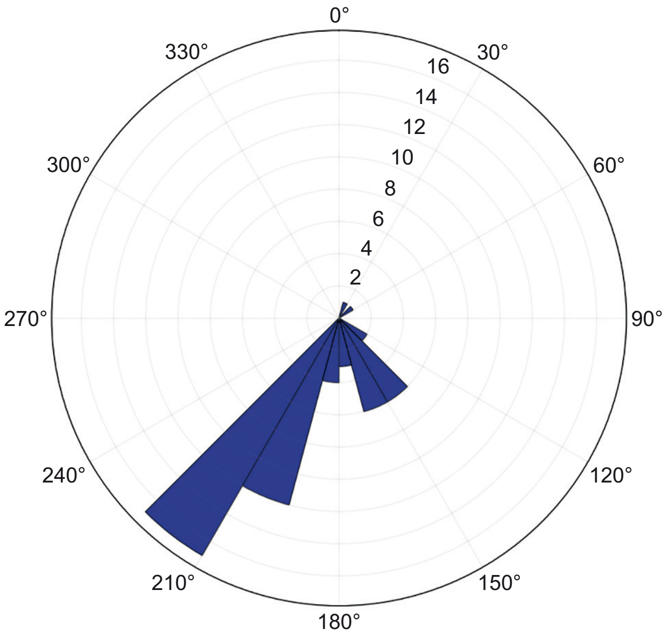


**Fig. 13.** Rose diagram of lineament orientations of the CVL.

**Рис. 13.** Роза-диаграмма направлений линеаментов Камерунской линии вулканов.

revealed are those of Eseka and the fault zone between Besoung Kang and the Mt. Kupe. Several faults can be found on both sides of the PAB. The faults clearly reveal that the PAB has gone through a series of uplifts and deformations which have produced many fracture zones in the area. There is also a fault system around the basement of the Mt. Cameroon and the Bioko Island which may be due to thrusting and uplifting because of volcanic and tectonic activities. The buried CCSZ that stretches from east to west in the study area possesses several faults that can be seen around Mamfe and Kajifa. At the extreme west of the study area, there are two lineaments representing breaks in the sedimentary crustal blocks. The alignment of newly identified lineaments with zones of microseismicity recorded along the CCSZ and FSZ provides independent evidence that these structures accommodate with the present day strain [Mbossi et al., 2026]. These results, combined with the spatial correlation to active volcanic centers (e.g., Mt. Cameroon), supports the interpretation of ongoing crustal deformation along the CVL, highlighted by mild to moderate seismicity in this zone [Noel et al., 2014].

## 5. CONCLUSION

This work revealed a dense network of lineaments, which provides new findings and proves the efficiency of the combined approach of utilizing gravity data (XGM2019 e_2159), magnetic data (EMAG2), and topographic data (GMRT) in analysing crustal structures of the CVL. Previous research has demonstrated the ability of derivative approaches to identify certain geologic structures when applied to gravity and magnetic field data. With the combination of 2D Laplace transformation on the DEM of the study area, it is possible to locate more lineaments. Some of the lineaments identified in this research coincide with old and well-known faults, thus indicating that old faults could still have stress and fracturing in those areas. This study identified 52 previously unmapped tectonic lineaments across the CVL, representing a significant expansion of the regional structural database. These newly delineated features are validated through: (i) multi-dataset coherence (gravity, magnetics, topography), (ii) correlation with instrumental seismicity, and (iii) 3D structural visualization highlighting lineament-bounded crustal blocks. This refined structural framework advances regional tectonic models of the CVL and provides a foundation for future geohazard and geothermal investigations. The result of this research is in alignment with different researchers who have concluded that the CVL is a highly fractured zone, and its tectonic system is still very active.

## 6. ACKNOWLEDGMENT

The work was carried out at the Faculty of Geology & Geophysics of Novosibirsk State University, Russia. The author expresses his gratitude to the university and the scientific supervisor for their tremendous support for assisting with the research environment and tools for this work.

## 7. DISCLOSURE

The author has no conflicts of interest to declare relevant to this manuscript. The author read and approved the final version.

## 8. REFERENCES

Adams A., 2022. Insights Into the Source of Magmatic Hot-Lines: Forty Years of Geophysical Studies of the Cameroon Volcanic Line. Frontiers in Earth Science 10, 838993. https://doi.org/10.3389/feart.2022.838993.

Begg G.C., Griffin W.L., Natapov L.M., O'Reilly S.Y., Grand S.P., O'Neill C.J., Hronsky J.M.A., Djomani Y.P., Swain C.J., Deen T., Bowden P., 2009. The Lithospheric Architecture of Africa: Seismic Tomography, Mantle Petrology, and Tectonic Evolution. Geosphere 5 (1), 23–50. https://doi.org/10.1130/GES00179.1.

Blakely R.J., 1996. Potential Theory in Gravity and Magnetic Applications. Cambridge University Press, 441 p.

Blakely R.J., Simpson R.W., 1986. Approximating Edges of Source Bodies from Magnetic or Gravity Anomalies. Geophysics 51 (7), 1494–1498. https://doi.org/10.1190/1.1442197.

Burke K., 2001. Origin of the Cameroon Line of Volcano-Capped Swells. The Journal of Geology 109 (3), 349–362. https://doi.org/10.1086/319977.

Castaing C., Feybesse J.L., Thiéblemont D., Triboulet C., Chèvremont P., 1994. Palaeogeographical Reconstructions of the Pan-African/Brasiliano Orogen: Closure of an Oceanic Domain or Intracontinental Convergence Between Major Blocks? Precambrian Research 69 (1–4), 327–344. https://doi.org/10.1016/0301-9268(94)90095-7.

Cheunteu Fantah C.A., Mezoue C.A., Mouzong M.P., Kamga A.P.T., Nouayou R., Nguiya S., 2022. Mapping of Major Tectonic Lineaments Across Cameroon Using Potential Field

Data. Earth Planets Space 74 (1), 59. https://doi.org/10.1186/s40623-022-01612-7.

Cooper G.R.J., Cowan D.R., 2008. Edge Enhancement of Potential-Field Data Using Normalized Statistics. Geophysics 73 (3), H1–H4. https://doi.org/10.1190/1.2837309.

Déruelle B., Moreau C., Nkoumbou C., Kambou R., Lissom J., Njonfang E., Ghogomu R.T., Nono A., 1991. The Cameroon Line: A Review. In: A.B. Kampunzu, R.T. Lubala (Eds), Magmatism in Extensional Structural Settings. Springer, Berlin, Heidelberg, p. 274–327. https://doi.org/10.1007/978-3-642-73966-8_12.

Déruelle B., Ngounouno I., Demaiffe D., 2007. The "Cameroon Hot Line" (CHL): A Unique Example of Active Alkaline Intraplate Structure in Both Oceanic and Continental Lithospheres. Comptes Rendus. Géoscience 339 (9), 589–600. https://doi.org/10.1016/j.crte.2007.07.007.

Dobretsov N.L., Vasilevskiy A.N., 2018. Gravity Field, Surface Topography, and Volcanic Complexes of Kamchatka and Its Junction with the Aleutian Arc. Russian Geology and Geophysics 59 (7), 780–802. https://doi.org/10.1016/j.rgg.2018.07.005.

Dorbath C., Dorbath L., Fairhead J.D., Stuart G.W., 1986. A Teleseismic Delay Time Study Across the Central African Shear Zone in the Adamawa Region of Cameroon, West Africa. Geophysical Journal International 86 (3), 751–766. https://doi.org/10.1111/j.1365-246X.1986.tb00658.x.

Dumont J.F., 1986. Remote Sensing Identification of the Sanaga Fault (Cameroon). Its Position in the Context of Major Faults in Central Africa and the Northern Limit of the Congo Craton. Geodynamics 1, 13–19.

Ebinger C.J., Keir D., Bastow I.D., Whaler K., Hammond J.O.S., Ayele A., Hautot S., 2017. Crustal Structure of Active Deformation Zones in Africa: Implications for Global Crustal Processes. Tectonics 36 (12), 3298–3332. https://doi.org/10.1002/2017TC004526.

Ekolle N., Vasilevskiy A., Esin E., 2025. Determination of 3D Gravity Source and Its Depth Beneath Cameroon Volcanic Line (CVL) Using DEXP Transformation. Russian Journal of Earth Sciences 25 (3), 1–21. https://doi.org/10.2205/2025ES000991.

Elsheikh A.A., Gao S.S., Liu K.H., 2014. Formation of the Cameroon Volcanic Line by Lithospheric Basal Erosion: Insight from Mantle Seismic Anisotropy. Journal of African Earth Sciences 100, 96–108. https://doi.org/10.1016/j.jafrearsci.2014.06.011.

Fairhead J.D., Okereke C.S., 1987. A Regional Gravity Study of the West African Rift System in Nigeria and Cameroon and Its Tectonic Interpretation. Tectonophysics 143 (1–3), 141–159. https://doi.org/10.1016/0040-1951(87)90084-9.

Fedi M., Florio G., 2001. Detection of Potential Fields Source Boundaries by Enhanced Horizontal Derivative Method. Geophysical Prospecting 49 (1), 40–58. https://doi.org/10.1046/j.13652478.2001.00235.x.

Fitton J.G., 1987. The Cameroon Line, West Africa: A Comparison Between Oceanic and Continental Alkaline Volcanism. Alkali Igneous Rocks. Geological Society of London Special Publications 30, 273–291. https://doi.org/10.1144/GSL.SP.1987.030.01.13.

Florio G., Fedi M., Pasteka R., 2006. On the Application of Euler Deconvolution to the Analytic Signal. Geophysics 71 (6), L87–L93. https://doi.org/10.1190/1.2360204.

Gautier K.P., Loudi Y., Alain Z.A., Ludovic K.H., Sévérin N., Joseph K., 2022. Evaluation of Global Gravity Field Models Using Shipborne Free-Air Gravity Anomalies over the Gulf of Guinea, Central Africa. Survey Review 54 (384), 243–253. https://doi.org/10.1080/00396265.2021.1921519.

Glukhmanchuk E.D., Vasilevskiy A.N., 2013. Description of Fracture Zones Based on the Structural Inhomogeneity of the Reflector Deformation Field. Russian Geology and Geophysics 54 (1), 82–86. https://doi.org/10.1016/j.rgg.2012.12.007.

Goussi Ngalamo J.F., Sobh M., Bisso D., Abdelsalam M.G., Atekwana E., Ekodeck G.E., 2018. Lithospheric Structure Beneath the Central Africa Orogenic Belt in Cameroon from the Analysis of Satellite Gravity and Passive Seismic Data. Tectonophysics 745, 326–337. https://doi.org/10.1016/j.tecto.2018.08.015.

Holden E.-J., Wong J., Wedge D., Martis M., Lindsay M., Gessner K., 2016. Improving Assessment of Geological Structure Interpretation of Magnetic Data: An Advanced Data Analytics Approach. Computers & Geosciences 87, 101–111. https://doi.org/10.1016/j.cageo.2015.11.010.

Jacobsen B.H., 1987. A Case for Upward Continuation as a Standard Separation Filter for Potential-Field Maps. Geophysics 52 (8), 1138–1148. https://doi.org/10.1190/1.1442378.

Kamguia J., Nouayou R., Tabod C.T., Tadjou J.M., Manguelle-Dicoum E., Kande H.L., 2008. Geophysical Signature of Geological Units Inferred from the Analysis of Geoid Maps in Cameroon and Its Surroundings. Journal of African Earth Sciences 52 (1–2), 1–8. https://doi.org/10.1016/j.jafrearsci.2008.02.002.

Kamto P.G., Adiang C.M., Nguiya S., Kamguia J., Yap L., 2020. Refinement of Bouguer Anomalies Derived from the EGM2008 Model, Impact on Gravimetric Signatures in Mountainous Region: Case of Cameroon Volcanic Line, Central Africa. Earth and Planetary Physics 4 (6), 639–650. http://doi.org/10.26464/epp2020065.

Kemgang Ghomsi F.E., Ribeiro-Filho N., Baldez R., Tenzer R., Martins C.M., Chisenga C., Nguiya S., Nouayou R., 2021. Identification of Cameroon's Geological Structures Through a Gravity Separation and Using Seismic Crustal Models. Journal of African Earth Sciences 173, 104027. https://doi.org/10.1016/j.jafrearsci.2020.104027.

Kenfack J.V., Kamguia J., Dongmo A.K., Kengni L., Mbog M.B., Tassongwa B., Tabod C.T., 2017. Estimation of the Depth of Major Subsurface Discontinuities Beneath the Mount Cameroon Region, Central Africa, Based on New and Existing Gravity Data Analysis. Earth Science Research 6 (1), 142. https://doi.org/10.5539/esr.v6n1p142.

Koumetio F., Njomo D., Tatchum C.N., Tokam A.P.K., Tabod T.C., Manguelle-Dicoum E., 2014. Interpretation of Gravity Anomalies by Multi-Scale Evaluation of Maxima of Gradients and 3D Modelling in Bipindi Region (South-West

Cameroon). International Journal of Geosciences 5 (12), 1415–1425. https://doi.org/10.4236/ijg.2014.512115.

Kovesi P., 2003. Phase Congruency Detects Corners and Edges. In: C. Sun, H. Talbot, S. Ourselin, T. Adriaansen (Eds), Digital Image Computing: Techniques and Applications. Proceedings of the VII Biennial Australian Pattern Recognition Society Conference, DICTA 2003 (December 10–12, 2003, Sydney). Vol. 1. CSIRO Publishing, p. 309–318.

Lawrence S.R., Munday S., Bray R., 2002. Regional Geology and Geophysics of the Eastern Gulf of Guinea (Niger Delta to Rio Muni). The Leading Edge 21 (11), 1112–1117. https://doi.org/10.1190/1.1523752.

MacLeod I.N., Jones K., Dai T.F., 1993. 3D Analytical Signal in the Interpretation of Total Magnetic Field Data at Low Magnetic Latitudes. Exploration Geophysics 24 (3), 679–688. https://doi.org/10.1071/EG993679.

Marcel J., Abate Essi J.M., Nouck P.N., Sanda O., Manguelle-Dicoum E., 2018. Validation of Gravity Data from the Geopotential Field Model for Subsurface Investigation of the Cameroon Volcanic Line (Western Africa). Earth, Planets and Space 70 (1), 42. https://doi.org/10.1186/s40623-018-0812-x.

Marzoli A., Piccirillo E.M., Renne P.R., Bellieni G., Iacumin M., Nyobe J.B., Tongwa A.T., 2000. The Cameroon Volcanic Line Revisited: Petrogenesis of Continental Basaltic Magmas from Lithospheric and Asthenospheric Mantle Sources. Journal of Petrology 41 (1), 87–109. https://doi.org/10.1093/petrology/41.1.87.

Maus S., Barckhausen U., Berkenbosch H., Bournas N., Brozena J., Childers V., Dostaler F., Fairhead J.D. et al., 2009. EMAG2: A 2–Arc Min Resolution Earth Magnetic Anomaly Grid Compiled from Satellite, Airborne, and Marine Magnetic Measurements. Geochemistry, Geophysics, Geosystems 10 (8), Q08005. https://doi.org/10.1029/2009GC002471.

Mbossi E.F., Ndibi E.D.D., Abate Essi J.M., Wokwenmendam P.N., Ntepe N., Meghraoui M., Ateba B., Tabod C.T., 2026. Seismotectonic Analysis and Characterization of Seismic Source Zones in Cameroon, Central Africa. Earthquake Science 39 (2), 156–189. https://doi.org/10.1016/j.eqs.2026.01.004.

Meyers J.B., Rosendahl B.R., Harrison C.G.A., Ding Z.-D., 1998. Deep-Imaging Seismic and Gravity Results from the Offshore Cameroon Volcanic Line, and Speculation of African Hotlines. Tectonophysics 284 (1–2), 31–63. https://doi.org/10.1016/S0040-1951(97)00173-X.

Miller H.G., Singh V., 1994. Potential Field Tilt – A New Concept for Location of Potential Field Sources. Journal of Applied Geophysics 32 (2–3), 213–217. https://doi.org/10.1016/0926-9851(94)90022-1.

Ming Y., Ma G., Li L., Han J., Wang T., 2021. The Spatial Different Order Derivative Method of Gravity and Magnetic Anomalies for Source Distribution Inversion. Remote Sensing 13 (5), 964. https://doi.org/10.3390/rs13050964.

Ndikum E.N., Tabod C.T., 2023. Regional Intrusive Signature from the Cameroon Coastal Basins to Bioko Island in Equatorial Guinea (Gulf of Guinea) Using Gravity Studies. Journal of Geoscience and Environment Protection 11 (1), 1–14. https://doi.org/10.4236/gep.2023.111001.

Ndougsa-Mbarga T., Layu D.Yu., Yene-Atangana J.Q., Tabod C.T., 2014. Delineation of the Northern Limit of the Congo Craton Based on Spectral Analysis and 2.5D Modeling of Aeromagnetic Data in the Akonolinga-Mbama Area, Cameroon. Geofísica Internacional 53 (1), 5–16. https://doi.org/10.1016/S0016-7169(14)71486-2.

Nguiya S., Cheunteu Fantah C.A., Nouayou R., 2018. Gravity Imaging of the Crustal Structures Beneath Southern Cameroon and Its Tectonic Implications. The International Journal of Engineering and Science 7 (8), 8–23. DOI:10.9790/1813-0708020823.

Noel E.O.R., Marcelin M.R., Bekoa A., 2014. Crustal Structure and Seismogenic Zone of Cameroon: Integrated Seismic, Geological and Geophysical Data. Open Journal of Earthquake Research 3 (4), 152–161. https://doi.org/10.4236/ojer.2014.34015.

Poudjom Djomani Y.H., Diament M., Wilson M., 1997. Lithospheric Structure Across the Adamawa Plateau (Cameroon) from Gravity Studies. Tectonophysics 273 (3–4), 317–327. https://doi.org/10.1016/S0040-1951(96)00280-6.

Rani R., Kumari S., 2016. A Review on Edge Detection Using Different Techniques. International Journal of Science and Research 5 (6), 2133–2137. https://doi.org/10.21275/v5i6.NOV164719.

Savant S., 2014. A Review on Edge Detection Techniques for Image Segmentation. International Journal of Computer Science and Information Technologies 5 (4), 5898–5900.

Serpelloni E., Vannucci G., Pondrelli S., Argnani A., Casula G., Anzidei M., Gasperini P., 2007. Kinematics of the Western Africa-Eurasia Plate Boundary from Focal Mechanisms and GPS Data. Geophysical Journal International 169 (3), 1180–1200. https://doi.org/10.1111/j.1365-246X.2007.03367.x.

Sumintadireja P., Dahrin D., Grandis H., 2018. A Note on the Use of the Second Vertical Derivative (SVD) of Gravity Data with Reference to Indonesian Cases. Journal of Engineering and Technological Sciences 50 (1), 127–139. https://doi.org/10.5614/j.eng.technol.sci.2018.50.1.9.

Tatchum C.N., Tabod C.T., Manguelle-Dicoum E., 2006. A Gravity Study of the Crust Beneath the Adamawa Fault Zone, West Central Africa. Journal of Geophysics and Engineering 3 (1), 82–89. https://doi.org/10.1088/1742-2132/3/1/009.

Tokam A.P.K., Tabod C.T., Nyblade A.A., Julià J., Wiens D.A., Pasyanos M.E., 2010. Structure of the Crust Beneath Cameroon, West Africa, from the Joint Inversion of Rayleigh Wave Group Velocities and Receiver Functions. Geophysical Journal International 183 (2), 1061–1076. https://doi.org/10.1111/j.1365-246X.2010.04776.x.

Toteu S.F., Penaye J., Poudjom D.Y., 2004. Geodynamic Evolution of the Pan-African Belt in the Central Africa with Special Reference to Cameroon. Canadian Journal of Earth Sciences 41, 73–85. https://doi.org/10.1139/e03-079.

Zingerle P., Pail R., Gruber T., Oikonomidou X., 2020. The Combined Global Gravity Field Model XGM2019e. Journal of Geodesy 94 (7), 66. https://doi.org/10.1007/s00190-020-01398-0.